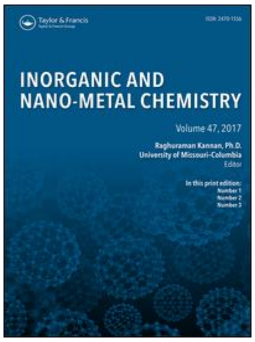

Inorganic and Nano-Metal Chemistry

ISSN: 2470-1556 (Print) 2470-1564 (Online) Journal homepage: https://www.tandfonline.com/loi/lsrt21

Synthesis, spectral and electrochemical studies of mononuclear samarium (II), europium (II) and ytterbium (II) complexes with a NNO donor Schiff base derived from 4-methyl-2,6-dibenzoylphenol and propane-1,3-diamine

Sanjay Kumar & Sushil K Gupta

To cite this article: Sanjay Kumar & Sushil K Gupta (2019): Synthesis, spectral and electrochemical studies of mononuclear samarium (II), europium (II) and ytterbium (II) complexes with a NNO donor Schiff base derived from 4-methyl-2,6-dibenzoylphenol and propane-1,3-diamine, Inorganic and Nano-Metal Chemistry, DOI: 10.1080/24701556.2019.1606828

To link to this article: https://doi.org/10.1080/24701556.2019.1606828

INORGANIC AND NANO-METAL CHEMISTRY
https://doi.org/10.1080/24701556.2019.1606828

Taylor & Francis
Taylor & Francis Group

Synthesis, spectral and electrochemical studies of mononuclear samarium (II), europium (II) and ytterbium (II) complexes with a NNO donor Schiff base derived from 4-methyl-2,6-dibenzoylphenol and propane-1,3-diamine

Sanjay Kumar and Sushil K Gupta

School of Studies in Chemistry, Jiwaji University, Gwalior, India

ABSTRACT

Three mononuclear divalent lanthanide complexes, $[Sm(L)_2(THF)_2]$ (**1**), $[Eu(L)_2(THF)_2]$ (**2**) and $[Yb(L)_2(THF)_2]$ (**3**), (where HL^{Me} = 2-{N-(3-aminopropyl)benzimidoyl}-6-benzoyl-4-methylphenol) have been synthesized and characterized by elemental analyses, conductivity measurements, mass spectrometry, IR, electronic and ^1H NMR spectroscopy and cyclic voltammetry. The spectral studies suggest that the LnN_4O_4 coordination polyhedron is a distorted dodecahedral. The electrochemical behavior of **1**–**3** shows irreversible metal centered oxidation wave at *ca.* 0.544–0.643 V and ligand centered reduction at *ca.* −1.085 to −1.260 V versus Ag/Ag^+. Interaction of **1**, **2** and **3** with calf thymus DNA suggests an intercalative binding mode.

ARTICLE HISTORY
Received 26 October 2018
Accepted 19 March 2019

KEYWORDS
Divalent lanthanides; NNO Schiff base; NMR; cyclic voltammetry; DNA binding

Introduction

Tridentate ligands such as phenol based compartmental Schiff base are capable of forming complexes that have important applications in several areas of research. Lanthanide-Schiff base complexes are receiving great attention for important catalytic and biological applications.[1–6] Generally, the tridentate Schiff base ligands with a flexible donor atom, in comparison with bidentate ligands, can provide the protective shield for catalytically active metal centers leading to a more stable active species by the coordination of the additional donor atom. As a result, the activity of the complex with a tridentate Schiff base ligand is much higher than that of complex with bidentate ligands.[7,8] Various divalent lanthanide complexes with cyclopentadienyl and pyrazolylborate ligands have been reported.[9–14] However, lanthanide complexes with phenol based tridentate Schiff base still remain poorly explored.[15] In repertoire, monomeric lanthanocene aryloxide complexes with a tridentate Schiff base ligands, N-1-(*o*-methoxyphenyl)salicylideneamine have been described.[16] As part of our research work on phenol-based Schiff bases,[17–21] we herein report the synthesis and characterization of divalent lanthanide complexes with tridentate NNO Schiff base, 2-{N-(3-aminopropyl)benzimidoyl}-6-benzoyl-4-methylphenol ($L^{Me}H$).

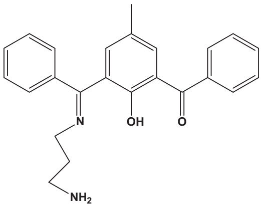

$L^{Me}H$

Experimental

Materials

All chemicals were of reagent grade and used as received. Solvents were purified by standard methods[22] and freshly distilled prior to use. Samarium(II) iodide, europium(II) bromide, ytterbium(II) iodide and propane-1,3-diamine were obtained from Aldrich. Calf thymus DNA was obtained from Sigma and used as received. The sodium salt of CT DNA was stored at 4 °C. Precursor, 4-methyl-2,6-dibenzoylphenol (mdbpH) was synthesized by a previously reported method.[17]

Physical measurements

Elemental analysis were carried on Elemental Vario EL analyzer model CARLO ERBA model DP 200. Molar conductance of the complex in 10^{-3} mol L^{-1} CH_3CN solution was measured by use of a Century CC-601 digital conductivity meter. Melting point was determined on a LABTRONICS model LT-110 Digital Automatic Melting Point Apparatus in an open capillary and are reported without further correction. The electrospray ion mass spectra (ESIMS) were recorded on a MICROMASS QUATTRO II triple quadrupole mass spectrometer. Infrared spectra were recorded on a KBr pellets using SHIMADZU Prestige-21 FT IR Instruments. Electronic spectra of 10^{-3} mol L^{-1} solutions in CH_3CN were obtained on a PerkinElmer Lambda 35 UV–vis spectrophotometer. ^1H NMR spectra were recorded on a 500 MHz JEOL AL-500 FT NMR spectrometer in $DMSO\text{-}d_6/CDCl_3$ relative to $SiMe_4$. The magnetic moment was measured on a Sherwood susceptibility instrument model MSB MK1 at room temperature.

CONTACT Sushil K Gupta skggwr@gmail.com School of Studies in Chemistry, Jiwaji University, Gwalior, 474 011, India.

Electrochemical experiments

Cyclic voltammetry

Cyclic voltammetric measurements were carried out with an Advanced Electrochemical System, PARSTAT 2253 instrument equipped with a three-electrode system. The micro-cell model KO264 consisted of a platinum working electrode, platinum wire as auxiliary electrode and a non-aqueous Ag/Ag$^+$ reference electrode with 0.1 mol L^{-1} $AgNO_3$ in acetonitrile as a filling solution. Tetrabutylammonium perchlorate (0.1 mol L^{-1} solution in CH_3CN) was used as the supporting electrolyte. Cyclic voltammograms with scan speeds of 50–500 mV s^{-1} were run in 10×10^{-3} mol L^{-1} CH_3CN solution under nitrogen. Under these conditions the ferrocenium/ferrocene (fc+/fc) couple shows $E^1\!/_2$ at 0.060 V.

DNA binding studies

Electronic absorption spectroscopy

The experiments involving the interaction of the complex with CT-DNA were carried out in doubly distilled water buffer containing 5 mM Tris [tris(hydroxymethyl)-aminomethane] and 50 mM NaCl and adjusted to pH 7.2 with hydrochloric acid. Solution of CT-DNA gave ratios of absorbance at 260 and 280 nm of about 1.8–1.9, indicating that the DNA was sufficiently free of protein contamination.[23] The DNA concentration per nucleotide was determined spectrophotometrically by employing a molar absorption coefficient of 6600 M^{-1}cm^{-1} at 260 nm after 1:100 dilutions.[24] The complex was dissolved in a solvent mixture of 1% DMSO and 99% Tris-HCl buffer (5 mM Tris-HCl, 50 mM NaCl, pH 7.2) at concentration 3.0×10^{-5} M. An absorption titration experiment was performed by maintaining 30 µM compound and varying the concentration of nucleic acid. While measuring the absorption spectra, an equal amount of CT-DNA was added to both the compound solution and the reference solution to eliminate the absorbance of CT-DNA itself. Titration curves were constructed from the fractional change in the absorption intensity as a function of DNA concentration. The intrinsic binding constant can be obtained by the following equation[25]:

$$[\mathrm{DNA}]/(\varepsilon_{a-}\varepsilon_f) = [\mathrm{DNA}]/(\varepsilon_{b-}\varepsilon_f) + 1/K_b(\varepsilon_{b-}\varepsilon_f) \tag{1}$$

In plots of [DNA]/(ε_a $_-$ ε_f) versus [DNA], K_b is given by the ratio of the slope to intercept.

Synthesis of tridentate Schiff base ligand

Synthesis of [2-{N-(3-aminopropyl)benzimidoyl}-6-benzoyl-4-methylphenol] ($L^{Me}H$)

The ligand precursor, $L^{Me}H$, was synthesized by a previously reported method[17] using 4-methyl-2,6-dibenzoylphenol and propane-1,3-diamine in dry THF at 0 °C.

Synthesis of complexes

[Bis(2-{N-(3-aminopropyl)benzimidoyl-NC}-6-benzoyl-4-methylphenolato-κ^3 N^{1}N^{2}O^1)(tetrahydrofuran- κ O) samarium(II)] [Sm(L^{Me})$_2$(THF)$_2$] (1)

To a solution of SmI_2 (0.328 g; 0.812 mmol) in THF (30 cm^3) was added drop-wise a solution of $L^{Me}H$ (0.603 g, 1.623 mmol) in THF (30 cm^3) at room temperature and the mixture was slowly heated at 50 °C for 1 hr. After cooling, a yellow precipitate was obtained, filtered and washed with cold THF and dried in vacuum. Yield: 0.464 g (64%), m.p. 265 °C (dec.). Anal. Calc. for $C_{56}H_{62}N_4O_6Sm$ (%): C, 64.83; H, 6.02; N, 5.40. Found: C, 64.95; H, 5.96; N, 5.51. ESI-MS: *m/z* (relative abundance, %): 728 (8) $[M–2THF–NH_2(CH_2)_3NH_2–PhCH_3]^+$, 671 (100) $[M–2THF–NH_2(CH_2)_3NH_2–PhCH_3–NH(CH_2)_3]^+]$, 437 (8) $[Sm(LH)-N(CH_2)_3NH_2-CH_3]^+$, 373 (12) $[LH + H]^+$, 356 (22) $[LH–CH_4]^+$, 317 (25) $[(2,6\text{-}PhCO)_2(4\text{-}Me)C_6H_2OH + H]^+$, 301 (20) $[MH - N(CH_2)_3NH_2-CH_2]^+$. FT IR (selected, cm^{-1}): 3056 [ν(N – H)]; 1637 [ν(C = O)]; 1572 [ν(C = N)/ring]; 1523 [$\nu(C\underline{\cdots}O)$/phenolate]; 1443 [$\delta$(C–H) bending/$CH_2$]; 1040 [$\nu$(C–O–C)]; 768 [$\rho(CH_2)$ rocking]; 522 [ν(Sm – N)]; 496 [ν(Sm – O)]. UV-Vis (nm) (ε/L mol^{-1}cm^{-1}) (CH_3OH): 413 (432), 262 (1213), 218 (2500). ^1H NMR (500 MHz, dmso-d_6): δ 1.54 (t, J = 6.5 Hz, CH_2); 2.70 (t, J = 6.5 Hz, CH_2); 3.60 (m, CH_2); 2.35 (s, CH_3), 2.50 (CH_2); 7.02 – 7.74 (m, aromatic); 8.11 (s, NH_2). Λ_M (10^{-4} M, MeOH, 298 K): 19 *S* cm^{2}mol^{-1}.

[Bis(2-{N-(3-aminopropyl)benzimidoyl}-6-benzoyl-4-methylphenolato-κ^{3}N^{1}N^{2}O^1) (tetrahydrofuran- κ O) europium(II)] [Eu(L^{Me})$_2$(THF)$_2$] (2)

A solution of $EuBr_2$ (0.316 g, 1.02 mmol) in THF (35 cm^3) was added drop-wise a solution of $L^{Me}H$ (0.752 g, 2.02 mmol) in THF (30 cm^3) at room temperature and the mixture was slowly heated at 50 °C for 1 hr. After cooling, a pale yellow precipitate was obtained, filtered and washed with cold THF and dried in vacuum. Yield: 0.532 g (59%), m.p. 277 °C (dec.). Anal. Calc. for $C_{56}H_{62}N_4O_6Eu$ (%): C, 64.73; H, 6.01; N, 5.39. Found: C, 64.65; H, 5.90; N, 5.46. ESI-MS: *m/z* (relative abundance, %): 805 (10) $[M–2THF–NH_2(CH_2)_3NH_2–CH_4]^+$, 728 (22) $[M–2THF–NH_2(CH_2)_3NH_2–Ph - CH_4]^+$, 709 (100) $[M–2THF–C_4H_5N_2-PhCO]^+$, 671 (40) $[MH–NH_2(CH_2)_3NH_2–PhCH_3–NH(CH_2)_3]^+$, 429 (8) $[EuLH - Ph - H_2O]^+$, 356 (22) $[LH - CH_4]$, 317 (25) $[(2,6\text{-}PhCO)_2(4\text{-}Me)C_6H_2OH + H]^+$, 301 (20) $[MH - N(CH_2)_3NH_2-CH_2]^+$. FT IR (selected, cm^{-1}): 3056 [ν(N – H)]; 1636 [ν(C = O)]; 1573 [ν(C = N)]; 1531 [ν(C = O)/phenolate]; 1464 [δ(C–H) bending/CH_2]; 1046 [ν(C–O–C)]; 704 [$\rho(CH_2)$ rocking]; 526 [ν(Eu – N)]; 498 [ν(Eu – O)]. UV-Vis (nm) (ε/L mol^{-1}cm^{-1}) (CH_3OH): 407 (713), 259 (1998), 208 (2748). Λ_M (10^{-4} M, MeOH, 298 K): 15 *S* cm^{2}mol^{-1}.

[Bis(2-{N-(3-aminopropyl)benzimidoyl}-6-benzoyl-4-methylphenolato-$\kappa^3N^1N^2O^1$) (tetrahydrofuran- κ O) ytterbium(II)] [Yb(L^{Me})$_2$(THF)$_2$] (3)

A solution of YbI_2 (0.326 g, 0.763 mmol) in THF (30 cm^3) was added drop-wise a solution of $L^{Me}H$ (0.565 g, 1.52 mmol) in THF (30 cm^3) at room temperature and the mixture was slowly heated at 50 °C for 1 hr. After cooling, a yellow precipitate was obtained, filtered and washed with cold THF and dried in vacuum. Yield: 0.489 g (70%), m.p. 256 °C (dec.). Anal. Calc. For $C_{56}H_{62}N_4O_6Yb$ (%): C, 63.44; H, 5.89; N, 5.28. Found: C, 63.30; H, 5.72; N, 5.34. ESI-MS: *m/z* (relative abundance, %): 917 (12) $[MH{-}2THF]^+$, 804 (48) $[M{-}2N(CH_2)_3]^+$, 723 (22) $[M{-}2N(CH_2)_3{-}C_4H_5N_2]^+$, 671 (40) $[M{-}2N(CH_2)_3{-}C_4H_5N_2{-}C_4H_4]^+$, 429 (12) $[YbLH-CPhCO]^+$, 357 (10) $[LH-CH_3]^+$, 317 (20) $[(2,6\text{-}PhCO)_2(4\text{-}Me)C_6H_2OH+H]^+$, 301 (10) $[MH-N(CH_2)_3NH_2{-}CH_2]^+$. FT IR (selected, cm^{-1}): 3020 [ν(N − H)]; 1633 [ν(C = O)]; 1573 [ν(C = N)/ν(C–C) ring]; 1526 [ν(C = O)/phenolate]; 1424 [δ(C–H) bending/CH_2]; 1050 [ν(C–O–C)]; 760 [ρ(CH_2) rocking]; 625 [ν(Yb − N)]; 489 [ν(Yb − O)]. UV-Vis (nm) (ε/L $mol^{-1} cm^{-1}$) (CH_3OH): 407 (456), 266 (1220), 218 (3022). ^1H NMR (500 MHz, $CDCl_3$): δ 2.77 (s, CH_2); 2.94 (s, CH_2); 3.34 (s, CH_2); 2.12 (s, CH_3), 6.01 − 7.38 (m, aromatic); 9.60 (s, NH_2). Λ_M (10^{-4} M, MeOH, 298 K): 14 *S* cm^2mol^{-1}.

Results and discussion

Synthesis and properties of lanthanide (II)-Schiff base complexes

The reactivity of the monoanionic tridentate ligand towards divalent lanthanide derivatives has been studied by reacting them in 1:2 molar ratio (Scheme 1). The products obtained are found to have composition $[M(L)_2(THF)_2]$ [M = Sm(**1**); Eu(**2**); Yb(**3**)] in good yield. All the complexes are stable at room temperature, soluble in acetonitrile, chloroform, methanol, DMSO and DMF and melt with decomposition in the temperature range 256 − 277 °C.

$$MX_2 \quad + \quad 2LH \xrightarrow[RT]{THF} [M(L)_2(THF)_2] \qquad M = Sm(\mathbf{1}), Eu(\mathbf{2}), Yb(\mathbf{3})$$

$$LH = [(6\text{-}PhCO)(4\text{-}Me)C_6H_2(OH)(2\text{-}CPh{=}N(CH_2)_3NH_2)]$$

Scheme 1. Preparation of complexes.

The molar conductance value in methanol is very low compared to the value reported[26] for 1:1 electrolyte (Λ_M 120 − 160 *S* cm^2 mol^{-1}) suggesting that these are non-electrolytes.

Mass spectra

All peaks in the electrospray mass spectra are identified by the most intense peak in the isotopic mass distribution. In compounds **1** and **2** the molecular ion peak was not observed. Peaks at *m/z* 728 (8%) and 883 (6%) are resulted from the loss of amine, toluene and carbon, respectively with typical isotopic pattern for samarium and europium. Other important peaks have similar fragmentation pattern as observed in the ligand. The ESI mass spectrum of **3** shows the expected molecular ion peak at *m/z* 916 with correct isotopic pattern of ytterbium. Other features are same as observed in case of **1** and **2**.

IR spectra

The absence of O – H stretching and δ(O – H) vibration (1270 cm^{-1}) in the IR spectra of complexes **1**, **2** and **3** indicated deprotonation of OH group.[27] The bands observed in the region 3020–3056 cm^{-1} in the complexes are assigned to ν(N–H) stretching. The lower value of ν(N–H) is attributed to the fact that the NH_2 group is coordinated to the metal. Further, the ν(C = N) vibration is shifted to lower frequency suggesting the coordination of azomethine N with lanthanide ions. However, the ν(C = O) band is found to be almost at the same position as in the precursor. This has been attributed to noninvolvement of benzoyl O in the coordination with lanthanide ion. The band at *ca.*1527 cm^{-1} has been assigned to ν(C = O) vibration of the phenol[28] as a consequences of the delocalization of the double bond. The presence of strong band in the region 1040–1050 cm^{-1} in **1**, **2** and **3** indicates coordinated THF [ν(C–O–C)].[29] This band appears at higher frequency in free THF (1086 cm^{-1}). The ligand coordination to the metal center results in bands at 522–625 cm^{-1}, ν(Ln–N) and at 489–496 cm^{-1}, ν(Ln–O).

Electronic spectra

The partially filled *f*-shell can participate in transitions in the visible region of the spectrum. For trivalent species, the colors arise from Laporte-forbidden 4*f* → 4f transitions.[30–32] In contrast, the colors of the divalent lanthanide ions are attributed to Laporte-allowed 4*f* → 5*d* transitions.[15] In the present investigations, the divalent lanthanide complexes **1**, **2**, and **3** in CH_3CN exhibit absorptions in the visible region. These low energy transitions (407–417 nm) are ascribed to ligand to metal charge transfer (LMCT)[33] transitions. In addition, all the complexes show very intense absorptions in the UV region (259–266; 208–218 nm), possibly due to intra-ligand transition (ILCT) as observed in the free ligands at similar energies.

^{1}H NMR spectra

Samarium (Sm) provides the only Ln(II)–Ln(III) system in which both oxidation states have complexes which are NMR accessible.[34] Despite room-temperature magnetic moments of 3.4–3.8 BM for Sm(II) ($4f^6$) and 1.3–1.9 BM for Sm(III) ($4f^5$), ^1H NMR resonances are reasonably sharp and are found within ± 10 ppm of the normal 0–10 ppm region where diamagnetic resonances are located. This is not true for Eu(II) ($4f^7$), Eu(III) ($4f^6$) or Yb(III) ($4f^{13}$), which have room temperature magnetic moment in the ranges 7.4–8.0, 3.3–4.2 and 4.2–4.9 BM, respectively.[35–37] Of course, diamagnetic Yb(II) ($4f^{14}$) (^{171}Yb, I = ½, abundance 14.27%) provides NMR-observable complexes.[38]

The ^{1}H NMR spectra of complexes **1** and **3** do not show any phenolic proton signal suggesting its displacement and coordination of phenolic oxygen with Sm(II) and Yb(II). The complexed THF proton appears at 0.83–0.88 and 2.43–2.58 ppm. The sharp spectrum of **3** compared to **1** confirmed the diamagnetic nature of ytterbium complex. Though the complex **1** is paramagnetic, however peaks have been assigned tentatively. The peaks for NH_2, CH_2, CH_3 and phenyl protons are observed in these complexes (see experimental section).

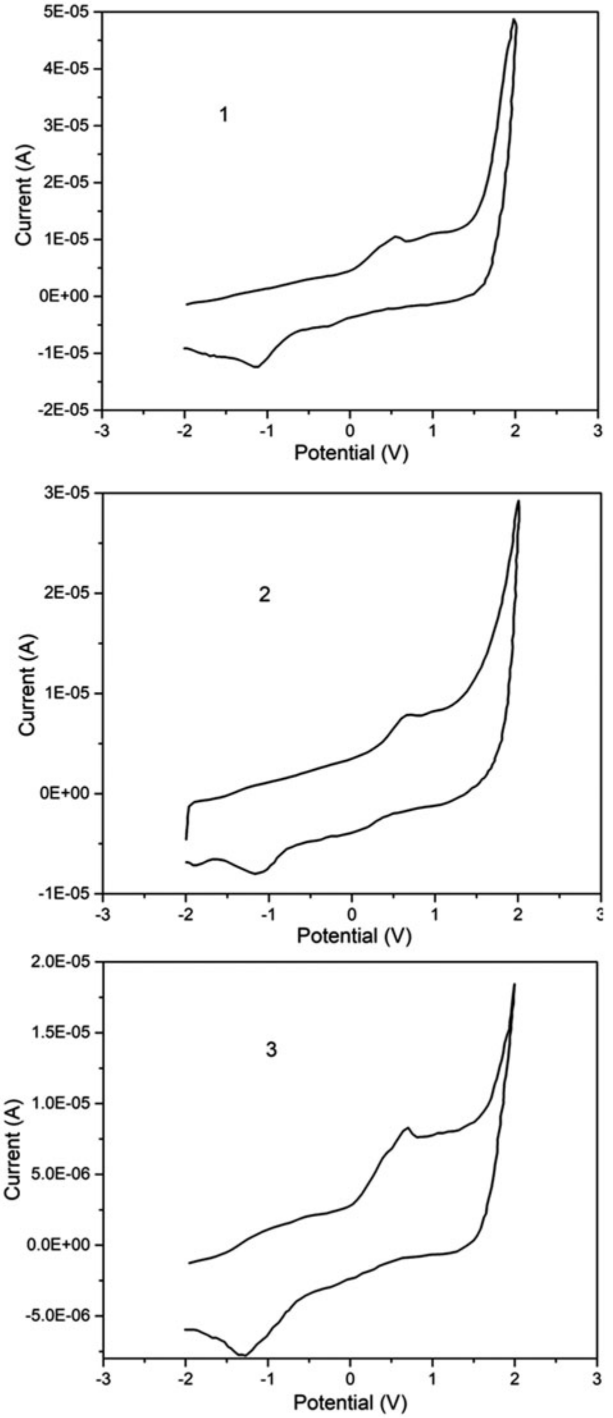

Figure 1. Cyclic voltammograms of 1, 2 and 3 (0.1 mM) in CH_3CN at 400 mV/s.

Table 1. Cyclic voltammetric data* for **1**, **2** and **3**.

Compound	Scan rate (mV/s)	E_{pa} (V)	i_{pa} (μA)	E_{pc} (V)	i_{pc}
1	50	0.472	2.268	−1.112	−2.504
	100	0.512	3.874	−1.072	−4.136
	150	0.544	5.092	−1.024	−6.062
	200	0.552	6.789	−1.024	−7.695
	250	0.576	7.436	−1.048	−9.059
	300	0.560	8.640	−1.088	−10.07
	350	0.560	9.781	−1.080	−11.42
	400	0.552	10.67	−1.096	−12.10
	450	0.560	11.69	−1.160	−12.93
	500	0.552	12.65	−1.152	−14.03
2	50	0.504	1.573	−1.112	−1.729
	100	0.560	2.704	−1.160	−2.883
	150	0.584	3.679	−1.112	−3.866
	200	0.600	4.796	−1.176	−5.076
	250	0.608	5.522	−1.104	−5.719
	300	0.624	6.321	−1.152	−6.603
	350	0.648	7.165	−1.128	−7.356
	400	0.656	7.790	−1.128	−7.919
	450	0.672	8.521	−1.112	−8.331
	500	0.688	9.194	−1.160	−9.197
3	50	0.512	2.058	−1.160	−2.092
	100	0.576	3.370	−1.184	−3.068
	150	0.584	4.219	−1.232	−4.126
	200	0.624	5.049	−1.248	−5.134
	250	0.632	5.940	−1.280	−5.762
	300	0.672	6.683	−1.264	−6.561
	350	0.696	7.521	−1.280	−7.208
	400	0.704	8.347	−1.296	−7.792
	450	0.696	9.080	−1.296	−8.398
	500	0.736	9.659	−1.352	−8.828

*Complex = 10×10^{-3} M in CH_3CN solution, supporting electrolyte: TBAP 0.1 M; working electrode: glassy carbon; auxiliary electrode: Pt wire; reference electrode: Ag/0.1 mol L^{-1} $AgNO_3$.

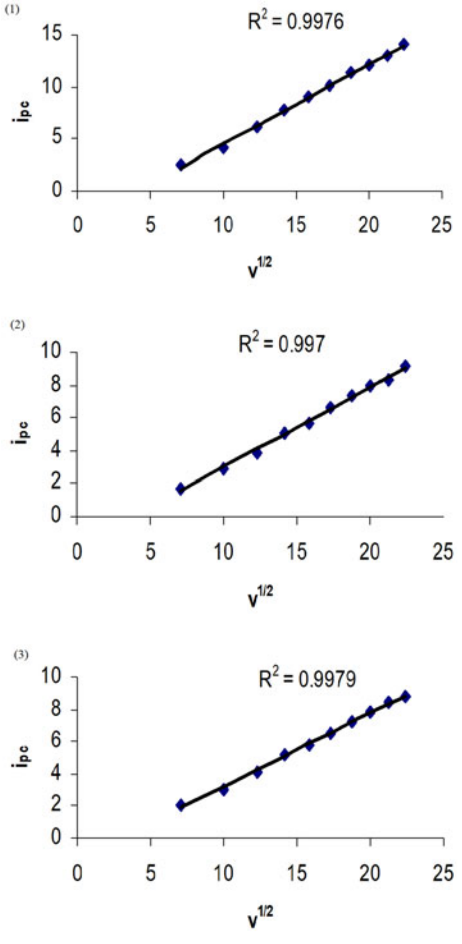

Figure 2. A plot of cathodic peak current (i_{pc}) vs square root of scan rate ($\nu^{1/2}$) of 1, 2 and 3.

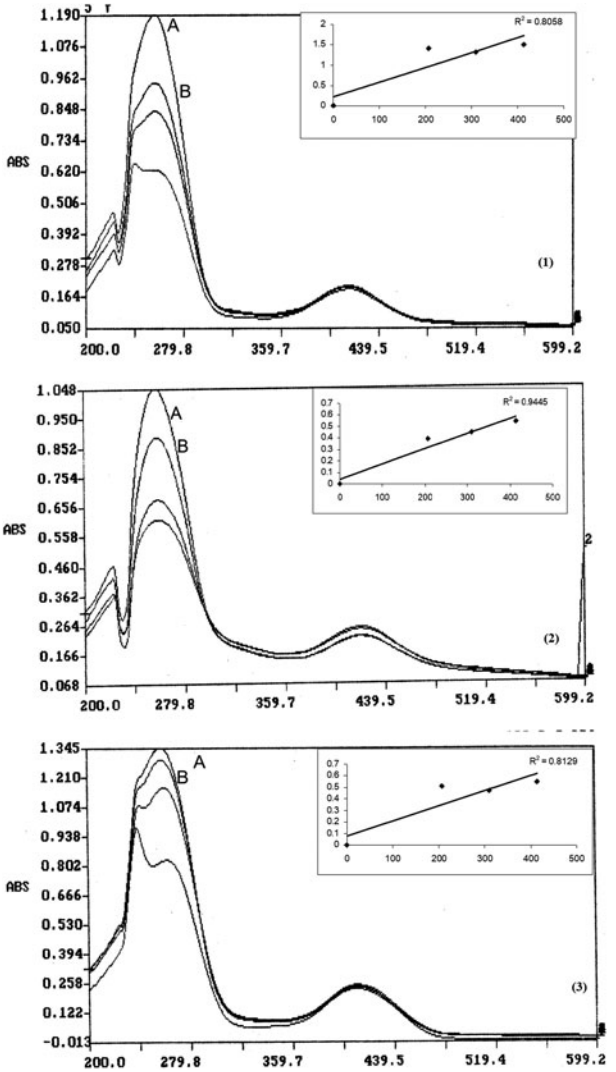

Figure 3. Absorption spectra of 30 μM [Complex] in the absence (a) and presence (b) of increasing amount of DNA (30–120 μM) for 1, 2 and 3. Inset shows the plot of [DNA]/($\varepsilon_a - \varepsilon_f$) versus [DNA].

Table 2. Absorption spectroscopic data of complexes **1**, **2** and **3** upon addition of CT DNA.

	λ_{max} (nm)				Binding constant,
Complexes	Free	Bound	$\Delta\lambda$	Hypochromism[a] (%)	K_b (M^{-1})
1	414	416	2	5.5	1.63×10^4
2	420	422	2	15.0	3.20×10^4
3	411	413	2	9.6	1.67×10^4

[a] Hypochromism = [(A $_{free}$ − A $_{bound}$)/A $_{free}$] × 100%.

Magnetic moment studies

The magnetic susceptibilities of lanthanide(II) complexes **1** and **2** in the solid state were determined by the Sherwood susceptibility instrument model MSB MK1 at room temperature (298 K). The experimental magnetic moments of the complex **1** is 3.65 BM and that of **2** is 8.20 BM which are comparable to the literature values.[34–37] Magnetic moment data reveal involvement of higher excited J states which made actual magnetic moments higher than those calculated by the use of Equation (1)[37] in Bohr magneton, with the value of J for the ground state (for Sm(II), $4f^6$, $\mu_{eff} = 0$ and for Eu(II), $4f^7$, $\mu_{eff} = 7.94$).

$$\mu_{eff} = g[J(J+1)]^{1/2} \qquad (1)$$

Cyclic voltammetry

The cyclic voltammograms of **1**, **2** and **3** showed a single wave at $E_{pa} = 0.552$ to 0.643 V *versus* the Ag/Ag^+ (Figure 1) in the 50–500 mV/s scan range (Table 1) attributable to an irreversible Ln^{2+}/Ln^{3+} one electron oxidation.[33,39,40] No cathodic peak could be observed even after applying a 500 mV/s scan rate indicating the irreversible nature of the electrode process. The linear plot of the cathodic peak current (I_{pc}) *versus* the square root of the scan rate ($\nu^{1/2}$) passes close to the origin, indicating that the electrode reaction is mainly diffusion controlled (Figure 2). An irreversible cathodic peak at $E_{pc} = -1.085$ to -1.259 V could be assigned to the reduction of the ligand[41] on the electrode surface (free ligand at *ca.* −1.173 V). The observed oxidation potential for the complexed Schiff base moiety with respect to the free ligand shows that the coordination to the electropositive lanthanide center facilitates the ligand reduction.

Efforts to grow a single crystal did not succeed, and this precluded a single crystal X-ray determination.

DNA binding properties

Electronic spectral studies

The UV-Vis spectra of the complexes **1**, **2** and **3** for a buffered solution at pH 7.2 in the presence of increasing quantities of CT DNA are shown in Figure 3. Absorption spectra exhibited hypochromism by 6 to 15% and moderate bathochromic shift in the charge transfer band of the complex (Table 2). The calculated values of binding constant (K_b) for the neutral complex $[Sm(L)_2(THF)_2]$ **1**, $[Eu(L)_2(THF)_2]$ **2** and $[Yb(L)_2(THF)_2]$ **3** at 30 μM are 1.63×10^4 M^{-1}, 3.20×10^4 M^{-1} and 1.67×10^4 M^{-1}, respectively. Addition of a 10–15 fold excess of CT DNA after saturation caused no change in the absorption spectrum of the final equilibrium mixture. It indicates an intercalative binding mode of complexes, possibly by electrostatic interaction with phosphate residues.[4–6,42]

Proposed structure of the complex

The analytical, spectral and electrochemical evidences suggest that complexes **1**, **2** and **3** have distorted dodecahedral geometry around the metal with tridentate coordination through amine N, imine N and phenolic O with tetrahydrofuran molecules occupying apical position in LnN_4O_4 core. Similar structure for complex $[Dy(bpdc)(Hbpdc)]\cdot 3H_2O]$ has earlier been reported.[43]

Funding

We are thankful to the Council of Scientific and Industrial Research (CSIR), New Delhi for financial support (Project no.01(1858)/03/EMR-II). SK acknowledges the CSIR for the award of JRF and SRF. We acknowledge CDRI, Lucknow for mass, NMR and CIF, JU for magnetic susceptibility measurements.

References

1. Datta, S.; Gamer, M. T.; Roesky, P. W. Aminotroponiminate Complexes of the Heavy Alkaline Earth and the Divalent Lanthanide Metals as Catalysts for the Hydroamination/Cyclization Reaction. *Organometallics* **2008**, *28*, 1207–1213. DOI: 10.1021/om701014d.
2. Bunzli, J.-C. G. Review: Lanthanide Coordination Chemistry: From Old Concepts to Coordination Polymers. *J. Coord. Chem.* **2014**, *67*, 3706–3733.
3. González-Lorenzo, M.; Platas-Iglesias, C.; Avecilla, F.; Geraldes, C. F. G. C.; Imbert, D.; Bünzli, J.-C. G.; de Blas, A.; Rodríguez-Blas, T. A Schiff-Base Bibracchial Lariat Ether Forming a Cryptand-like Cavity for Lanthanide Ions. *Inorg. Chem.* **2003**, *42*, 6946–6954. DOI: 10.1021/ic034024t.
4. Jiang, B.; Wang, M.; Li, C.; Xie, J. DNA-Binding and Hydrolytic Cleavage Promoted by Tetraazamacycle La(III) and Ce(III) Complexes. *Med. Chem. Res.* **2013**, *22*, 3398–3404. DOI: 10.1007/s00044-012-0357-7.
5. Moksharagni, B.; Reddy, K. H. Spectral Characterization and DNA Binding Properties of Lanthanide(III) Complexes with 2-Acetylpyridine Isonicotinoylhydrazone (APINH). *Bull. Chem. Soc. Eth.* **2016**, *30*, 221–230. DOI: 10.4314/bcse.v30i2.6.
6. Nayak, A. K.; Mishra, A.; Jena, B. S.; Mishra, B. K.; Subudhi, U. Lanthanum Induced B-to-Z Transition in Self-Assembled Y-Shaped Branched DNA Structure. *Sci. Rep.* **2016**, *6*, 26855DOI: 10.1038/srep26855.
7. Cameron, P. A.; Gibson, V. C.; Redshaw, C.; Segal, J. A.; White, A. J. P.; Williams, D. J. Synthesis and Characterisation of Neutral and Cationic Alkyl Aluminium Complexes Bearing *N*, *O*-Schiff Base Chelates with Pendant Donor Arms. *J. Chem. Soc, Dalton Trans.* **2002**, 415–422. DOI: 10.1039/b106131n.
8. O'Reilly, R. K.; Gibson, V. C.; White, A. J. P.; Williams, D. J. Design of Highly Active Iron-Based Catalysts for Atom Transfer Radical Polymerization: Tridentate Salicylaldiminato Ligands Affording near Ideal Nernstian Behavior. *J. Am. Chem. Soc.* **2003**, *125*, 8450–8451. DOI: 10.1021/ja035458q.
9. Evans, W. J. The Importance of Questioning Scientific Assumptions: Some Lessons from f Element Chemistry. *Inorg. Chem.* **2007**, *46*, 3435–3449. DOI: 10.1021/ic062011k.
10. Evans, W. J.; Bloom, I.; Hunter, W. E.; Atwood, J. L. Organolanthanide Hydride Chemistry. 3. Reactivity of Low-Valent Samarium with Unsaturated Hydrocarbons Leading to a Structurally Characterized Samarium Hydride Complex. *J. Am. Chem. Soc.* **1983**, *105*, 1401–1403.
11. Evans, W. J.; Ulibarri, T. A.; Ziller, J. W. Isolation and X-Ray Crystal Structure of the First Dinitrogen Complex of an f-Element Metal, $[(C_5Me_5)_2Sm]_2N_2$. *J. Am. Chem. Soc.* **1988**, *110*, 6877–6879. DOI: 10.1021/ja00228a043.
12. Liebing, P.; Kühling, M.; Takats, J.; Hilfertb, L.; Edelmann, F. T. Formation and Structural Characterization of a Europium(II) Mono(Scorpionate) Complex and a Sterically Crowded Pyrazabole. *Acta Crystallogr. E Cryst. Commun.* **2017**, *E73*, 1921–1925. DOI: 10.1107/S2056989017016498.
13. Arikawa, Y.; Inada, K.; Onishi, M. Side-on Coordination Mode of a Pyrazolyl Group in the Structure of a Divalent [Sm{B(3-Mepz)4}2] Complex (3-Mepz Is 3- Ethylpyrazol-1-yl. *Acta Cryst.* **2016**, *C72*, 838–841.
14. Palumbo, C. T.; Ziller, J. W.; Evans, W. J. Structural Characterization of the Bent Metallocenes, $[C_5H_3(SiMe_3)_2]_2Sm$ and $[C_5H_3(CMe_3)_2]_2Ln$ (Ln ¼ Eu, Sm), and the Mono(Cyclopentadienyl) Tetraphenylborate Complex, $[C_5H_3(CMe_3)_2]$ Eu(μ-η^6: η^1-Ph)$_2$BPh$_2$. *J. Organomet. Chem.* **2018**, *867*, 142–148. DOI: 10.1016/j.jorganchem.2017.09.038.
15. Molloy, J. K.; Philouze, C.; Fedele, L.; Imbert, D.; Jarjayes, O.; Thomas, F. Seven-Coordinate Lanthanide Complexes with a Tripodal Redox Active Ligand: structural, Electrochemical and Spectroscopic Investigations. *Dalton Trans.* **2018**, *47*, 10742–10751. DOI: 10.1039/C8DT01165F.
16. Yousaf, M.; Liu, Q. C.; Huang, J. L.; Qian, Y. L.; Chan, A. S. C. Synthesis and X-Ray Crystal Structure of Monomeric Lanthanocene Aryloxide Complexes with a Tridentate Schiff Base Ligand. *Inorg. Chem. Commun.* **2000**, *3*, 105–106. DOI: 10.1016/S1387-7003(00)00021-6.
17. Gupta, S. K.; Hitchcock, P. B.; Kushwah, Y. S. The Crystal Structure of 4-Methyl-2,6-Dibenzoylphenol and Its Conversion into a Mononuclear Cobalt(III) Complex by Treatment with Cobalt(II) Chloride and Propane-1,3-Diamine. *Polyhedron* **2002**, *21*, 1787–1793. DOI: 10.1016/S0277-5387(02)01044-6.
18. Gupta, S. K.; Hitchcock, P. B.; Kushwah, Y. S.; Argal, G. S. Synthesis, Structure and DNA Binding Studies of a Mononuclear Cobalt(III) Complex with a NNO Donor Schiff Base Derived from 4-Methyl-2,6-Dibenzoylphenol and Ethane-1,2-Diamine. *Inorg. Chim. Acta* **2007**, *360*, 2145–2152.
19. Gupta, S. K.; Hitchcock, P. B.; Argal, G. S. The Effect of Diamine Chain Length on the Formation of CoIII Schiff Base Complexes: The Unexpected Formation of a Neutral Complex Containing a Tetradentate Ligand. *Inorg. Chim. Acta* **2008**, *361*, 2139–2146. DOI: 10.1016/j.ica.2007.10.037.
20. Gupta, S. K.; Anjana, C.; Sen, N.; Butcher, R. J.; Jasinski, J. P.; Golen, J. A. An Unusual Hydroxy-Substituted Mononuclear Nickel(II) Complex with a Tetradentate Schiff Base: Synthesis, Spectroscopy, Electrochemistry, Crystallography, DNA Binding, and Theoretical Investigation. *Polyhedron* **2015**, *89*, 219–231. DOI: 10.1016/j.poly.2015.01.017.
21. Gupta, S. K.; Sen, N.; Ganaie, J. A.; Butcher, R. J.; Jasinski, J. P. Unusual Coordination of Mononuclear Cobalt(III) Complexes with Sterically Demanding Schiff Bases: synthesis, Spectroscopy, Electrochemistry, Crystallography, DNA Binding, and Theoretical Investigation. *J. Coord. Chem.* **2017**, *70*, 3147–3170. DOI: 10.1080/00958972.2017.1380196.
22. Armarego, W. L. F.; Perin, D. D. *Purification of Laboratory Chemicals*, 4th ed.; Butterworth-Heinemann, Oxford, **1997**.
23. Marmur, J. A Procedure for the Isolation of Deoxyribonucleic Acid from Micro –Organisms. *J. Mol. Biol.* **1961**, *3*, 208–218. DOI: 10.1016/S0022-2836(61)80047-8.
24. Reichmann, M. F.; Rice, S. A.; Thomas, C. A.; Doty, P. A Further Examination of the Molecular Weight and Size of Desoxypentose Nucleic Acid. *J. Am. Chem. Soc.* **1954**, *76*, 3047–3053. DOI: 10.1021/ja01640a067.
25. Wolfe, A.; Shimer, G. H.; Meehan, T. Polycyclic Aromatic Hydrocarbons Physically Intercalate into Duplex Regions of Denatured DNA. *Biochemistry* **1987**, *26*, 6392–6396. DOI: 10.1021/bi00394a013.
26. Geary, W. J. The Use of Conductivity Measurements in Organic Solvents for the Characterisation of Coordination Compounds. *Coord. Chem. Rev.* **1971**, *7*, 81–122. DOI: 10.1016/S0010-8545(00)80009-0.
27. Faniran, J. A.; Patel, K. S.; Bailar, J. C. Infrared Spectra of N,N'-Bis (Salicylidene) - 1,1 -(Dimethyl) Ethylenediamine and Its Metal Complexes. *J. Inorg. Nucl. Chem.* **1974**, *36*, 1547–1551. DOI: 10.1016/0022-1902(74)80621-4.
28. Mandal, S. K.; Nag, K. Dinuclear Metal Complexes. Part 2. Synthesis, Characterisation, and Electrochemical Studies of Macrocyclic Dicopper(II) Complexes. *J. Chem. Soc, Dalton Trans.* **1983**, 2429–2434. DOI: 10.1039/dt9830002429.
29. Nakamoto, K. *Infrared and Raman Spectra of Inorganic and Coordination Compounds*, 5th ed.; Wiley: New York, **1997**.
30. Moeller, T. In *Comprehensive Inorganic Chemistry*, J. C. Bailar, Jr. ed.; Pergamon Press: Oxford, **1973**, 4.
31. Mishra, S. N.; Sommerer, S. O. Absorption Spectra of Lanthanide Complexes in Solution. *Appl. Spect. Rev* **1991**, *26*, 151–202. DOI: 10.1080/05704929108050880.
32. Dieke, G. H. In Spectra and Energy Levels of Rare Earth Ions in Crystals, H. M. Crosswhite and H. Crosswhite, eds.; Wiley: New York, **1968**.

33. Carnall, W. T. In *Handbook on the Physics and Chemistry of Rare Earths*, K. A. Gschneidner Jr. and L. Ering, eds.; Elsevier: Amsterdam, **1979**.
34. Evans, W. J.; Bloom, I.; Hunter, W. E.; Atwood, J. L. Synthesis and X-Ray Crystal Structure of a Soluble Divalent Organosamarium Complex. *J. AM. Chem. Soc.* **1981**, *103*, 6507–6508. DOI: 10.1021/ja00411a046.
35. Cotton, S. A.; Hart, F. A. *The Heavy Transition Elements*, Wiley: New York, **1975**.
36. Cary, D. R.; Arnold, J. Synthesis and Characterization of Divalent Lanthanide Selenolates and Tellurolates. X-Ray Crystal Structures of Yb[SeSi(SiMe$_3$)$_3$]$_2$(TMEDA)$_2$ and {Eu[TeSi(SiMe$_3$)$_3$]$_2$(DMPE)$_2$)$_2$(M-DMPE). *Inorg. Chem.* **1994**, *33*, 1791–1796. DOI: 10.1021/ic00087a012.
37. Hamer, A. M.; Livingstone, S. E. The Magnetic Moments and Electronic Spectra of Lanthanide Chelates of 2-Thenoyltrifluoroaceton**e**. *Transition Met. Chem.* **1983**, *8*, 298–304. DOI: 10.1007/BF00620875.
38. Avent, A. G.; Edelman, M. A.; Lappert, M. F.; Lawless, G. A. The First High Resolution Direct NMR Observation of an f-Block Element. *J. Am. Chem. Soc.* **1989**, *111*, 3423–2425. DOI: 10.1021/ja00191a047.
39. Camp, C.; Guidal, V.; Biswas, B.; Pécaut, J.; Dubois, L.; Mazzanti, M. Multielectron Redox Chemistry of Lanthanide Schiff-Base Complexes. *Chem. Sci.* **2012**, *3*, 2433–2448.
40. Dyke, J. M.; Hush, N. S. A Spectroscopic Study of Eu(III)/Eu(II) and Sm(IlI)/Sm(II) Solutions in Acetonitrile Obtained by Controlled-Potential Reduction. *J. Electroanal. Chem.* **1972**, *36*, 337–347. DOI: 10.1016/0368-1874(72)80096-0.
41. Dube, T.; Gambarotta, S.; Yap, G. Preparation and Reactivity of a Compartmental Schiff-Base Samarium Dinuclear Complex. *Organometallics* **1998**, *17*, 3967–3973. DOI: 10.1021/om9803319.
42. Sharma, S.; Chandra, M.; Pandey, D. S. New Multifunctional Complexes [Ru(κ^3-L)(EPh$_3$)$_2$Cl]$^+$ [E = P, as; L = 2,4,6-Tris(2-Pyridyl)-1,3,5-Triazine] Containing Both Group V and Polypyridyl Ligands. *Eur. J. Inorg. Chem.* **2004**, *2004*, 3555–3563. DOI: 10.1002/ejic.200400069.
43. Liu, C.-M.; Zhang, D.-Q.; Hao, X.; Zhu, D.-B. Simultaneous Assembly of Mononuclear and Dinuclear Dysprosium(III) Complexes Behaving as Single-Molecule Magnets in a One-Pot Hydrothermal Synthesis. *Sci. China Chem.* **2017**, *60*, 358–365. DOI: 10.1007/s11426-016-0359-x.